

# Wideband RCS Reduction of Fabry-Perot Resonator Antenna Based on Diffuse Scattering Method

Guoqiang Feng and Peng Xie\*

*Air Force Engineering University, Xi'an, Shaanxi, China*

**ABSTRACT:** Three methods to reduce the RCS of Fabry-Perot (FP) resonator antenna using diffuse scattering are verified and compared in this paper. They are 1 bit random coding, 2 bit random coding, and 2 bit random phase gradient coding method. In order to realize reflection phase coding, a receiver-transmitter type unit with adjustable reflection phase from top side is proposed. Metasurface (MS) composed of this unit is the best choice to achieve the RCS reduction of FP resonator antenna, because it has the ability to independently control the reflection phase on both sides. By changing the size of radiation patch, two units with  $90^\circ$  reflection phase difference and four units with  $90^\circ$  reflection phase difference from top side can be obtained. They are used to compose MSs with different reflection phase distributions. These MSs can form FP resonator antennas with RCS reduction characteristics. Subsequently, three antennas are fabricated and tested, and the test results are compared. The results show that the FP resonator antenna using 2-bit random phase gradient coding has the best performance. It achieves the wideband RCS reduction of antenna and has the least influence on radiation performance. The proposed antenna A3 achieves an average RCS reduction of 12 dB over the bandwidth range of 7.7–13.7 GHz while maintaining a peak gain of 18 dB and good radiation patterns.

## 1. INTRODUCTION

Fabry-Perot (FP) resonator antenna is a very commonly used high-gain antenna with a simple structure. It usually consists of a feed antenna and a partial reflector plate. The distance between the above two is determined by the following formula [1].

$$\varphi_1 + \varphi_2 - \frac{4\pi h}{\lambda_0} = 2N\pi, \quad N = 0, 1, 2, \dots \quad (1)$$

There are often many metal structures distributed on partial reflector plate of the antenna. These metal structures are highly reflective of incoming electromagnetic waves, which causes the antenna to exhibit large radar cross-section (RCS) [2–4]. Therefore, it is necessary to take some measures to reduce the RCS of FP resonator antenna. This can help the antenna achieve radar stealth [5–8].

The common method to reduce the RCS of FP resonator antenna is to change the reflection phase of the partial reflector plate to the external incident electromagnetic wave. Through the reflection phase control, the reflected electromagnetic wave phases cancel each other, so that the reflected beam is divided into several beams in different directions or generates diffuse scattering. Thus, the intensity of the main reflected beam is reduced, and the RCS reduction is realized [9–14]. There are two kinds of reflection phase distribution commonly used. One is chessboard distribution [15–21], and the other is random coding distribution [22–27]. The chessboard distribution can divide the reflected electromagnetic wave into several beams. For example, a chessboard arranged metamaterial superstrate

is constructed using two different frequency selective surface (FSS) units for wideband gain enhancement and RCS reduction in [19]. The RCS was reduced from 8.0 to 18.0 GHz for arbitrary polarizations, including the operation band of antenna. This design method provides a good strategy to address the conflict between radiation and scattering performance of FP resonator antenna. In [20], an FP resonator antenna with RCS reduction performance using receiver-transmitter metasurface (MS) is presented. The antenna can realize wideband RCS reduction for both polarizations while maintaining good radiation performance. The random coding distribution method can form a diffuse reflection of the incident electromagnetic wave, i.e., the incident electromagnetic wave is reflected in many directions, so that the electromagnetic wave in each direction is very small, and thus achieves the reduction of RCS. For example, a strategy to realize a diffusion MS was proposed for RCS reduction in [24]. The designed MS effectively suppressed the backward RCS within the frequency range of 7.2–15.6 GHz. In [25], a specially designed 2-bit coding MS is introduced to reduce the scattering of FP antenna. Measured results indicated that it can effectively reduce the monostatic and bistatic RCSs of the FP resonator antenna. Comparing these two methods, diffuse scattering method can achieve better RCS reduction effect. But it also has a great effect on the radiation of the antenna.

In this paper, three methods to reduce the RCS of FP resonator antenna by diffuse scattering are compared. They are 1 bit random coding, 2 bit random coding, and 2 bit random phase gradient coding. The 1 bit random coding is a random arrangement of two types units whose reflection phases from top side differ by  $180^\circ$ . There are not many cell types required for this approach, and it is easy to implement. Therefore, it is a

\* Corresponding author: Peng Xie (xpcademic@163.com).

common method to achieve RCS reduction. The 2-bit random coding is random arrangement of four types units whose reflection phases from top side are  $90^\circ$  different in turn, while the random phase gradient coding forms a  $4 \times 4$  array with phase gradient firstly using these four types of units, and then the phase gradient direction of each array is arranged randomly to make up the MS. The 2-bit method requires four cell types and is difficult to implement. Random coding arrangements are relatively simple. The phase gradient coding method requires a detailed design of the unit arrangement. All three methods can achieve RCS reduction of antenna. However, the performance of RCS reduction and its effect on antenna radiation need further study. The RCS reduced FP resonator antenna realized by these three methods is simulated and tested, and their radiation and scattering characteristics are compared. The rest of this paper is arranged in the following order. The design process of the unit used to achieve reflection phase control is given in Section 2. Then, Section 3 mainly introduces the design process of three kinds of MS and the composition of FP resonator antenna. The simulation and test results of three antennas and the analysis of the results are presented in Section 4. Finally, Section 5 gives the conclusion of this paper.

## 2. DESIGN OF THE UNIT

In order to realize the RCS reduction of the FP resonator antenna, the partially reflective surface (PRS) of the antenna should present constant reflection coefficients from bottom side and adjustable reflection coefficients from top side. So a receiver-transmitter unit is designed to compose the PRS because it is easy to realize independent control of reflection coefficients from different sides. The configuration of the unit is shown in Figure 1. The unit consists of two identical substrates stacked up and down. The material of the substrate is F4B with relative permittivity of 2.65 and thickness of 1.6 mm. Three layers of metal structures are printed on the surfaces of two substrates. The top and bottom layers are both square patches. Bottom layer patch is the receiver, and top layer patch is the radiator. Two patches are separated by an all-metal surface on the middle layer, which acts as a ground plane. A rectangular slot is etched on the ground plane to realize the energy transmission from receiver to radiator. When the unit is working, the electromagnetic wave is received by the bottom layer patch and coupled to the top layer patch through the slot on the ground plane. Then the top layer patch radiates electromagnetic wave into free space. The unit is simulated by the CST, and the simulation model is presented in Figure 1(b). The reflection coefficients from port 1 and port 2 represent the reflection coefficients of unit from bottom and top sides, respectively. The transmissivity of the unit is related to the length of the slot. The longer the slot is, the smaller the impedance is, resulting in a larger transmissivity of the unit, while the size of the patch can not only influence the operating frequency but also affect the reflection phase of the unit. The dimensions of each part of the unit are determined in the following order. Firstly, the receiver and transmitter patches are set to the same size, and the operating frequency of the unit is adjusted to 10 GHz through tuning

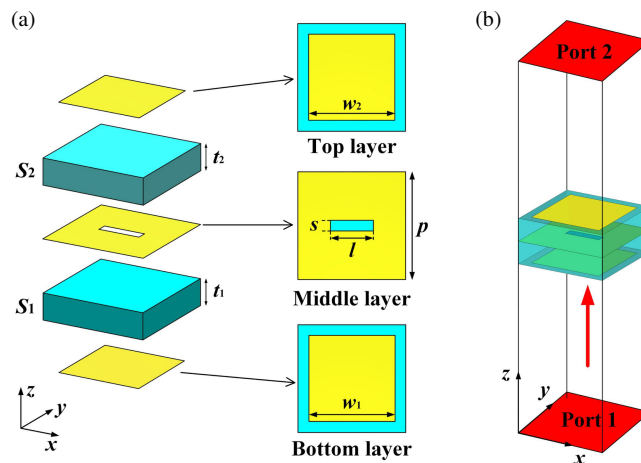


**FIGURE 1.** (a) Configuration of the proposed unit, and (b) the simulation model of the unit.

the width of patches. After simulation, the widths of patches are set to  $w_1 = w_2 = 6.2$  mm.

Secondly, the transmissivity and reflectivity of the unit are adjusted by changing the length of the coupling slot. The length of the slot manipulates the transmission amplitude mainly by affecting the coupling impedance. When the length of the slot  $l = 3$  mm and width  $s = 0.8$  mm, the reflectivity of the unit reaches above 0.9. The high reflectivity meets the requirements of the FP resonator antenna. Then, in order to realize the RCS reduction of the antenna, the reflection phase of the unit from top side must be tunable to obtain phase difference between different units. The width of the radiator patch can affect the reflection phase from the top side but not influence the reflection phase from bottom side. The increase of the width makes the transmission path of the reflected electromagnetic wave longer, resulting in the reflection phase lag, and vice versa. So, reflection phase of the unit from top side can be tuned by changing the width of the radiator patch  $w_2$ .

Figure 2 and Figure 3 show the reflection coefficients of unit from port 1 and port 2 with different values of  $w_2$ . Figure 2 displays the reflection coefficients of the unit at 10 GHz with  $w_2 = 5.37$  mm and 6.69 mm, while Figure 3 shows that with  $w_2 = 4.15$  mm, 5.92 mm, 6.45 mm, and 7.28 mm. Figure 2(a) and Figure 3(a) are the reflection coefficients of the unit from port 1. We can see that the change of  $w_2$  has very little influence on the reflection amplitude and phase from port 1. This is because the reflection coefficients from port 1 mainly depends on the size of receiver patch due to the existence of the ground plane. The reflection phases of the unit from port 2 with different values of  $w_2$  are shown in Figure 2(b) and Figure 3(b). From Figure 2(b), when  $w_2$  is equal to 5.37 mm and 6.69 mm, respectively, the reflection phases of unit from port 2 present  $180^\circ$  phase difference. These two units can be used to make up the MS with 1 bit coding of reflection phase. According to Figure 3(b), the reflection phase of the unit differs by  $90^\circ$  in turn when  $w_2$  is equal to 4.15 mm, 5.92 mm, 6.45 mm, and 7.28 mm. Thus, these four units can be used to form the MS with 2 bit coding of reflection phase. According to the simulation results, the unit proposed in this paper can not only keep

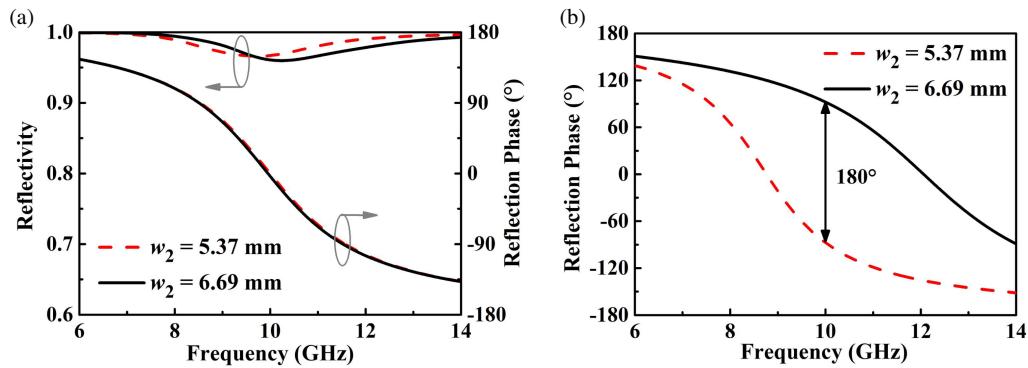


FIGURE 2. Reflection coefficients of unit with different value of  $w_2$  from (a) port 1 and (b) port 2.

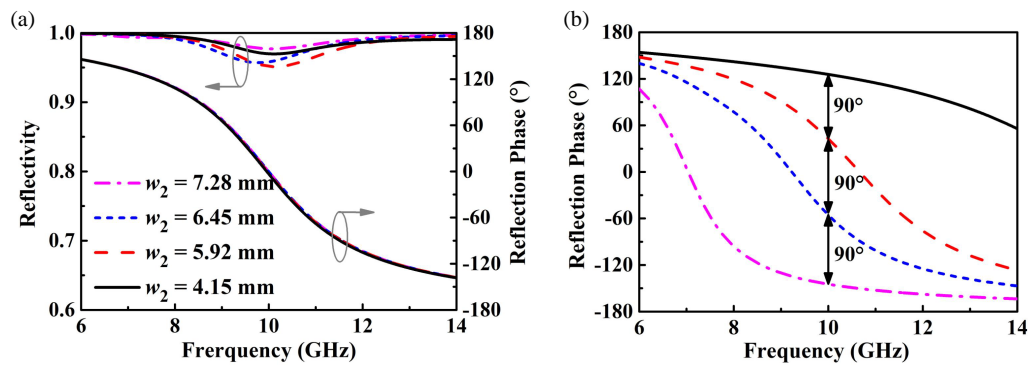


FIGURE 3. Reflection coefficients of unit with different value of  $w_2$  from (a) port 1 and (b) port 2.

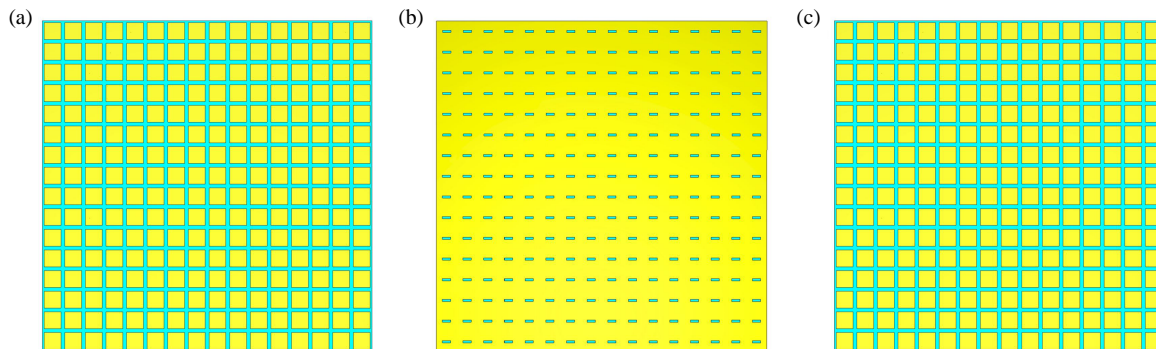


FIGURE 4. Detailed views of three layers of the MS. (a) Top layer, (b) middle layer, and (c) bottom layer.

the reflection coefficient from bottom side unchanged, but also adjust the reflection phase from top side by changing the size of the radiator patch, so as to realize the RCS reduction design of the antenna. The test results of the units are also shown in Figure 2 and Figure 3. Because a  $16 \times 16$  unit array is used for testing, the test results of the unit are slightly different from the simulation results. However, this does not affect the simulation results as the actual reflection and transmission coefficients of the unit.

### 3. THE FP RESONATOR ANTENNA

The proposed unit can be used to form the receiver-transmitter MS, which can present constant reflection coefficient from bot-

tom side and tunable reflection phase from top side. This MS is very conducive to form the FP resonator antenna. Figure 4 shows the three-layer structure of the MS consisting of the proposed units. The MS consists of  $16 \times 16$  units, whose radiator patches have the same size and are equal to the size of receiver patch. This MS is used as a prototype to design the FP resonator antenna. A slot coupled patch antenna is designed to act as the feeder of the FP resonator antenna. The sketch model of the patch antenna is shown in Figure 5. The antenna's operating frequency is adjusted to 10 GHz. Then an FP resonator antenna is formed by the MS and the feed antenna. The MS is placed above the antenna with a distance of  $h$ , which is the height of the resonator cavity. Four units are removed from each corner of the MS, and four through holes are opened to accommodate

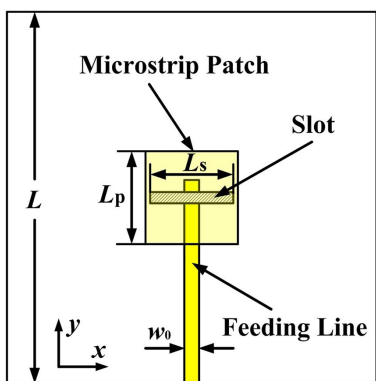


FIGURE 5. Sketch model of the feed antenna.

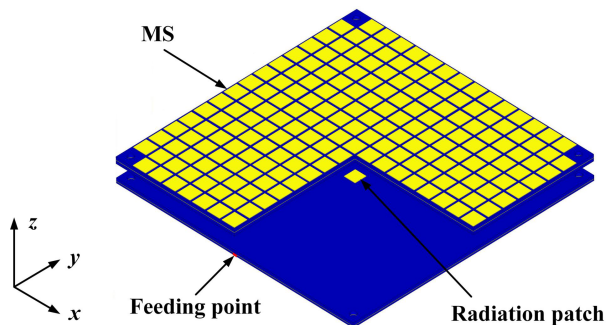


FIGURE 6. 3D view of the FP resonator antenna.

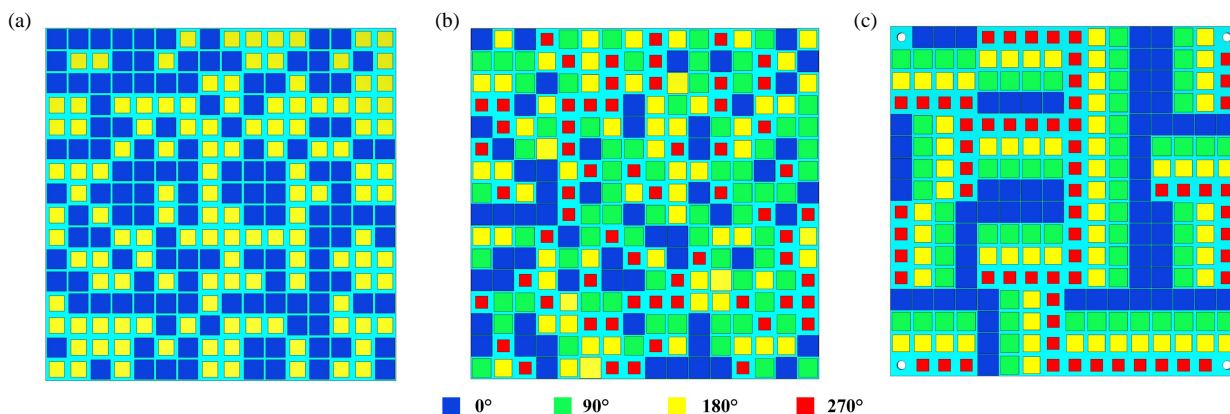


FIGURE 7. Top layers of three kind MSs. (a) 1 bit random coding, (b) 2 bit random coding, and (c) 2 bit random phase gradient coding.

the support structure. Figure 6 shows a model of the formed FP resonator antenna. The model of the formed FP resonator antenna is simulated by CST. The value of  $h$  is set to 5.5 mm after being optimized. At this point, the antenna can work well at 10 GHz.

Next, the MS needs to present uneven reflection phase distribution from top side to obtain RCS reduction property. According to the simulation results of the unit, the reflection phase from top side of each unit on the MS can be tuned by changing

the width of the radiator patch. In this paper, the diffuse scattering method is used to achieve RCS reduction. The diffuse scattering of incident electromagnetic wave is realized by three methods, which are 1 bit random coding, 2 bit random coding, and random phase gradient coding. The 1 bit random coding method uses two units with  $180^\circ$  reflection phase difference to compose the MS. According to the simulation results, the width of the radiation patch of the unit is 5.37 mm and 6.69 mm, respectively. Two units are arranged randomly on the MS to achieve diffuse scattering of incident waves. Figure 7(a) shows the top view of the 1 bit random coding MS. This method uses only two types of units and is relatively simple to implement. The method of 2-bit random coding is to make up the MS by randomly arranging 4 units whose reflection phases are  $90^\circ$  different with each other. The widths of the radiation patch of four units are 4.15 mm, 5.92 mm, 6.45 mm, and 7.28 mm. Top view of the 2 bit random coding MS is presented in Figure 7(b). The random phase gradient coding method also uses 4 units with  $90^\circ$  reflection phase difference to form the MS. The whole MS is divided into 16 parts, each containing  $4 \times 4$  units. Inside each part, the units are arranged in a gradient according to the reflection phase. There are four directions of the reflection phase gradient,  $+x$ ,  $-x$ ,  $+y$ , and  $-y$ . Then, the phase gradients of different parts are arranged randomly. Compared with random coding, this method has both randomness and regularity in unit arrangement. The top view of the random phase gradient cod-

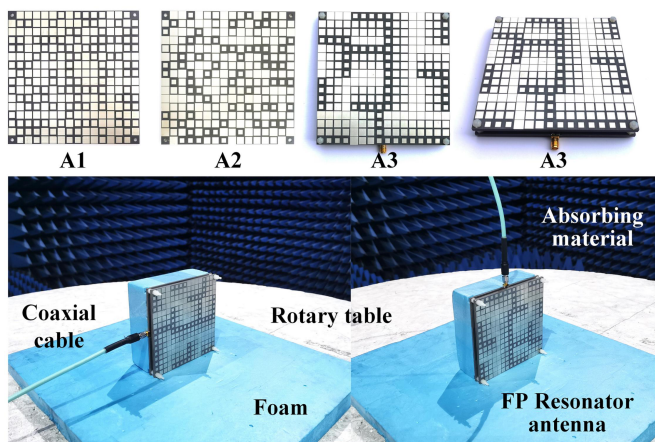
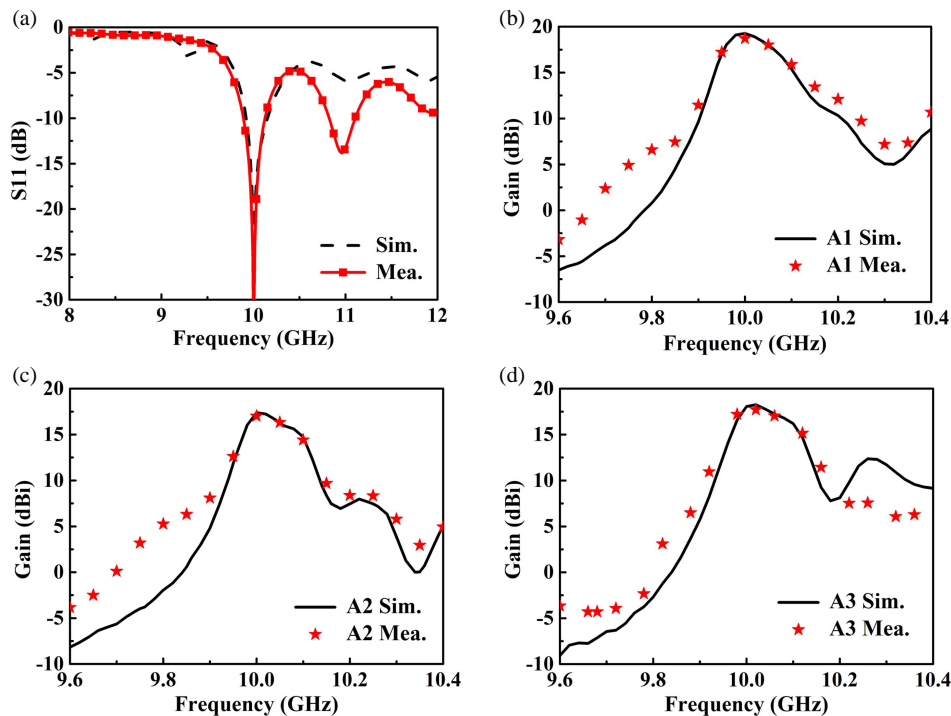


FIGURE 8. Fabricated antennas and the test environment.





**FIGURE 9.** Simulated and measured results of the antennas. (a) Reflection coefficients, (b) gain of A1, (c) gain of A2, and (d) gain of A3.

ing MS is shown in Figure 7(c). The receiver patch and ground planes of these three MSs are identical. So, the change of the radiation patch on MS does not affect the reflection coefficients of the MS.

#### 4. COMPARISON OF THREE ANTENNAS

According to theoretical analysis, all three methods can make the antenna realize RCS reduction. In order to compare the performance of three methods to achieve RCS reduction, three kinds of MS and feed antenna are machined and assembled to three FP resonator antennas. They are named A1, A2, and A3. Figure 8 shows the photographs of the fabricated antennas and the test environment.

The reflection coefficients and realized gains of antennas are displayed in Figure 9. Figure 9(a) shows the simulated and measured reflection coefficients of the antennas. Because three antennas have nearly the same reflection coefficient, the results of only one antenna are given in Figure 9(a). The test results agree well with the simulation ones. The reflection coefficient of the antenna in the range of 9.88–10.12 GHz is less than  $-10$  dB. The simulated and measured gains of three antennas are presented in Figures 9(b), (c), and (d). The tested maximum gains of antenna A1, A2, and A3 are 18.9 dBi, 17.1 dBi, and 18.0 dBi, respectively. Compared with the method of 1 bit random coding, the gain of 2 bit random coding antenna decreases more seriously. This is because when the size of the radiation patch is changed, the transmission phase of the unit also changes. The increase of the unit types on the surface of MS makes the transmission phase more uneven, which affects the radiation characteristics of the antenna. Although the random phase gradient coding is also composed of four types of units,

the unit arrangement on the random phase gradient coding MS has a certain regularity, so its influence on the antenna radiation characteristics is less than that of the 2 bit random coding method. Therefore, the gain of antenna A3 is between those of antennas A1 and A2.

The radiation patterns of the antennas are shown in Figure 10. The simulation and test results maintain a good consistency. It can be seen that antenna A1 presents the best radiation pattern. Its side lobe level and cross-polarization level are all below  $-15$  dB. Radiation patterns of the antenna using 2 bit random coding MS are relatively poor, which is manifested in that the main beam of the antenna is deformed, and the back lobe of the antenna is also larger. For antenna A3, the pattern of  $xoz$  plane is deteriorated, and the side lobe level is larger, but the pattern of  $yoze$  plane maintains good characteristics, and the side lobe level and cross polarization electricity are below  $-13$  dB on average. In summary, the radiation pattern of A1 is the best, and that of A2 is the worst, while that of A3 is between the first two.

In order to verify the RCS reduction property of the antenna, the monostatic RCS of the antenna was measured in an anechoic chamber. The measurement results are given in Figure 11. Figures 11(a), (c), and (e) are the RCS reduction performance of antennas A1, A2, and A3 under the incident condition of  $x$ -polarized wave, while (b), (d), and (f) are the RCS reduction performance under the incident condition of  $y$ -polarized wave. It can be seen that the RCS reduction performance of each antenna under the incident of  $x$ - and  $y$ -polarized waves is not different. Simulation and test results show that the RCS reduction performance of 2 bit random coding is better than that of 1 bit random coding, while random gradient phase coding is better than that of 2 bit random coding. The specific performance is

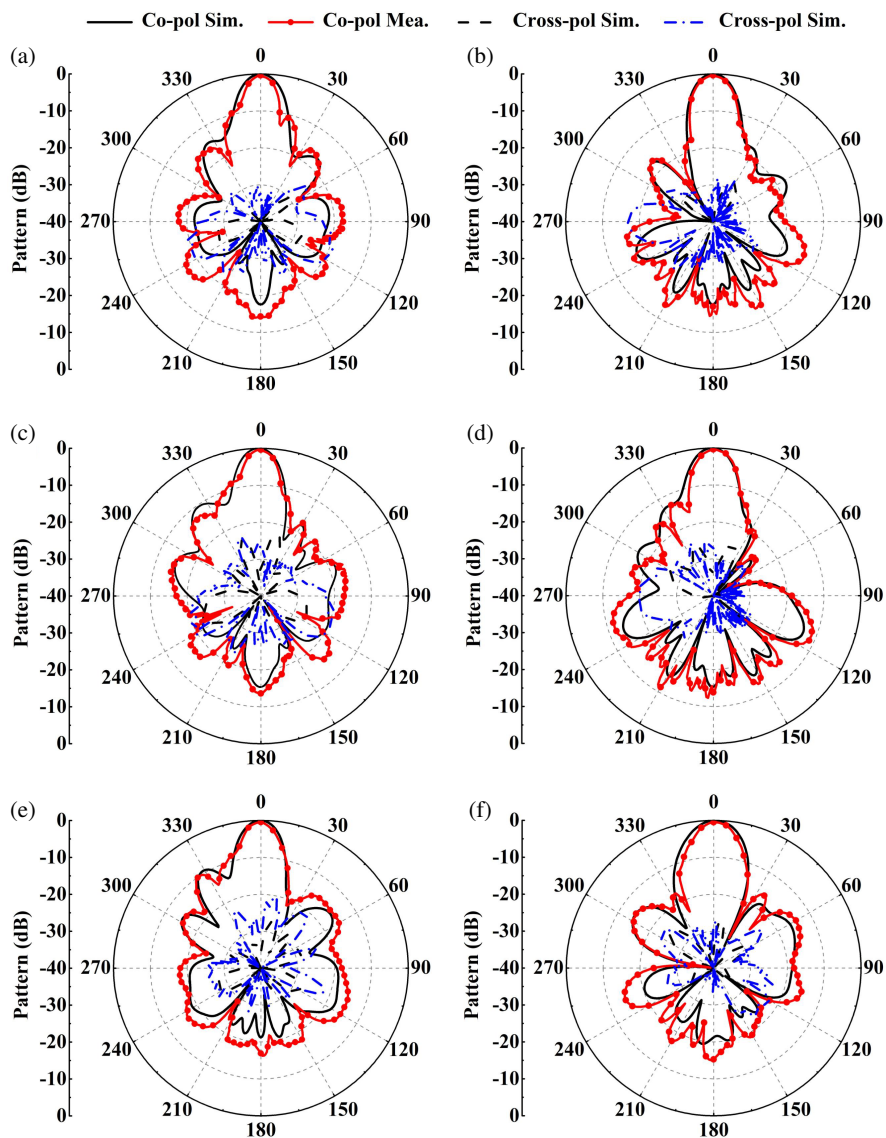


**FIGURE 10.** Radiation patterns of three antennas. (a) A1 in  $xoz$  plane, (b) A1 in  $yo z$  plane, (c) A2 in  $xoz$  plane, (d) A2 in  $yo z$  plane, (e) A3 in  $xoz$  plane, and (f) A3 in  $yo z$  plane.

**TABLE 1.** Comparison of the RCS reduction FP resonator antenna.

Ref.	Frequency (GHz)	Peak gain (dBi)	RCS reduction Band	Average RCS reduction	Overall Dimensions	Aperture Efficiency
[19]	10.4	11	8–18 GHz	10 dB	$2.2\lambda \times 2.2\lambda$	20.0%
[20]	10	18.2	8–14 GHz	10 dB	$4.3\lambda \times 4.3\lambda$	28.9%
[25]	10	19.8	8–12 GHz	8.76 dB	$3.6\lambda \times 3.6\lambda$	55.5%
A3 in this paper	10	18	7.7–13.7 GHz	12 dB	$4.3\lambda \times 4.3\lambda$	27.6%

that the bandwidth to achieve the RCS reduction effect is wider, and the RCS reduction at each frequency point is also larger. Therefore, considering the radiation characteristics and scattering characteristics of the antenna, antenna A3 achieves the best RCS reduction effect and has less influence on antenna gain. The RCS reduction of A3 is large than 12 dB in 7.7–13.7 GHz, and the in-band RCS reduction is greater than 15 dB.

The performance comparison between the proposed antenna and former reported RCS reduction FP resonator antenna is shown in Table 1. The RCS reduction property can be reflected by RCS reduction band and average RCS reduction, while the peak gain and aperture efficiency reflect the extent to which the radiation performance of the antenna is affected. It can be seen that the A3 proposed in this paper and other FP resonator an-

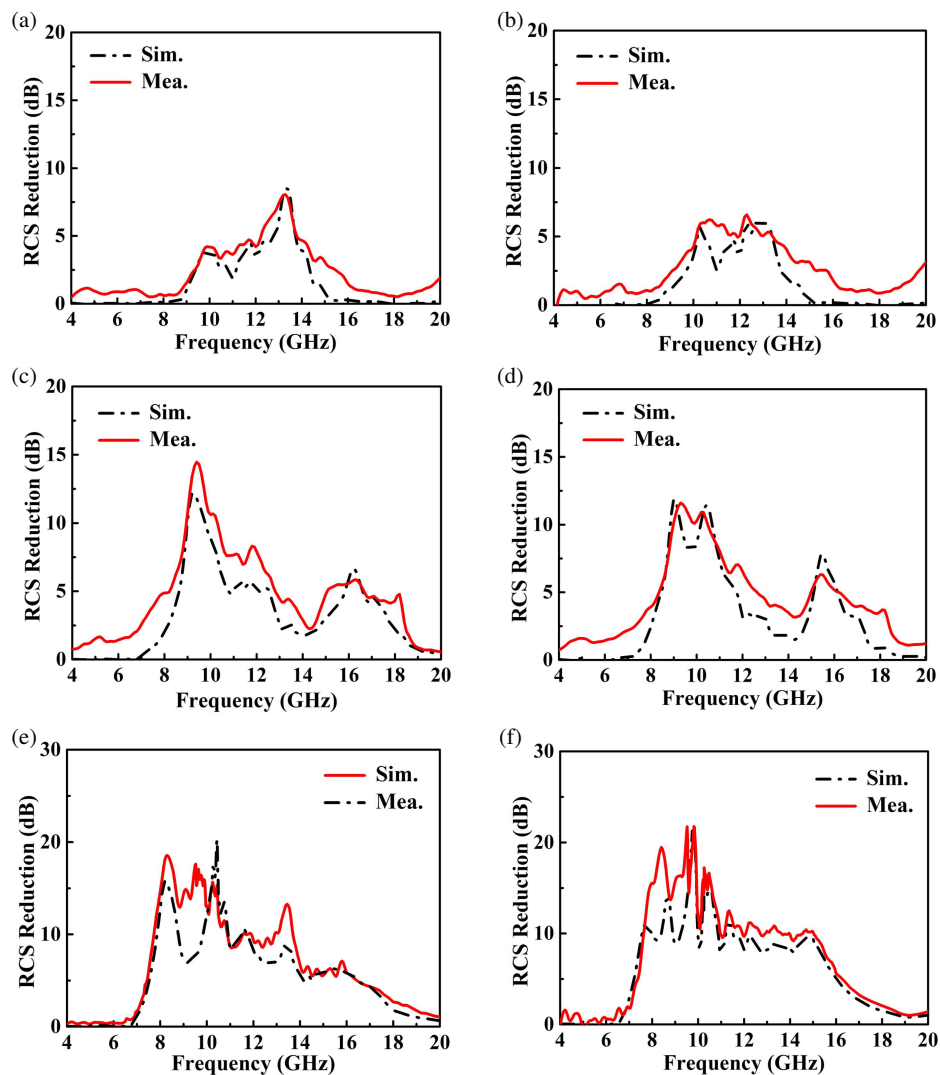


**FIGURE 11.** RCS reduction of three antennas. (a) A1 under  $x$ -polarized incident wave, (b) A1 under  $y$ -polarized incident wave, (c) A2 under  $x$ -polarized incident wave, (d) A2 under  $y$ -polarized incident wave, (e) A3 under  $x$ -polarized incident wave, and (f) A3 under  $y$ -polarized incident wave.

tennas in references can all realize wideband RCS reduction. The average RCS reduction of A3 is larger than other antennas, and the peak gain and aperture efficiency of A3 did not drop very much. This shows that the radiation performance of A3 is maintained well.

## 5. CONCLUSION

In this paper, three kinds of method to reduce the RCS of the FP resonator antenna are proposed, and their performances are compared. Firstly, a coupling type receiver-transmitter unit is designed, whose reflection phase from top side can be adjusted as needed. Then, two units with  $180^\circ$  reflection phase difference are used to compose the 1 bit random coding MS, and four units with  $90^\circ$  reflection phase difference with each other are used to form the 2 bit random coding MS and the 2 bit random phase gradient coding MS. The 1 bit random coding requires fewer types of units and is easy to implement. On the other

hand, the 2-bit method requires four cell types and is difficult to implement. Random coding arrangements are relatively simple. The phase gradient coding method requires a detailed design of the unit arrangement. Three kinds of MSs can all realize RCS reduction of the FP resonator antenna. However, the radiation characteristics of the antenna are affected in different degrees. Then, through the comparison of simulation and test results, the radiation and scattering characteristics of the antenna using three methods are analyzed. Compared with 1-bit random coding, 2-bit random coding can achieve better RCS reduction, but it also has greater influence on antenna radiation characteristics. This indicates that the more types of reflection phases of MS units str, the better the reduction effect of RCS is. The 2-bit random phase gradient coding method also uses 4 units with different reflection phases, but different units are arranged according to certain rules. Therefore, this method can achieve better RCS reduction effect and less influence on antenna radiation. Above all, the 2-bit random phase gradient coding is the

best way to reduce the RCS of FP resonator antenna. It enables FP resonator antenna to achieve an average RCS reduction of 12 dB over a wide bandwidth range.

## ACKNOWLEDGEMENT

This work was supported by the National Natural Science Foundation of China under Grant 62201610.

## REFERENCES

- [1] Trentini, G. V., "Partially reflecting sheet arrays," *IEEE Transactions on Antennas and Propagation*, Vol. 4, No. 4, 666–671, Oct. 1956.
- [2] Zou, Y., X. Kong, Z. Cao, X. Zhang, and Y. Zhao, "Reconfigurable integrated structures with functions of Fabry-Perot antenna and wideband liquid absorber for radar system stealth," *Scientific Reports*, Vol. 13, No. 1, 14678, 2023.
- [3] Xie, P., G. Wang, X. Zou, and B. Zong, "Gain and AR improvements of the wideband circularly polarized Fabry-Perot resonator antenna," *IEEE Transactions on Antennas and Propagation*, Vol. 69, No. 10, 6965–6970, Oct. 2021.
- [4] Liu, X., Z. Yan, E. Wang, T. Zhang, and F. Fan, "Magnetolectric dipole-fed Fabry-Perot antenna with wideband RCS reduction based on multilayer metasurface," *IEEE Antennas and Wireless Propagation Letters*, Vol. 20, No. 7, 1342–1346, Jul. 2021.
- [5] Ren, J., W. Jiang, K. Zhang, and S. Gong, "A high-gain circularly polarized Fabry-Perot antenna with wideband low-RCS property," *IEEE Antennas and Wireless Propagation Letters*, Vol. 17, No. 5, 853–856, May 2018.
- [6] Pan, W., C. Huang, P. Chen, X. Ma, C. Hu, and X. Luo, "A low-RCS and high-gain partially reflecting surface antenna," *IEEE Transactions on Antennas and Propagation*, Vol. 62, No. 2, 945–949, Feb. 2014.
- [7] Gan, L., W. Jiang, Q. Chen, X. Li, and Z. Zhou, "Analysis and reduction on in-band RCS of Fabry-Perot antennas," *IEEE Access*, Vol. 8, 146 697–146 706, Aug. 2020.
- [8] Huang, H.-F. and Q.-S. Fan, "Broadband and high-aperture efficiency Fabry-Perot antenna with low RCS based on nonuniform metamaterial superstrate," *Progress In Electromagnetics Research M*, Vol. 101, 59–68, 2021.
- [9] Zorbakhsh, S., M. Akbari, F. Samadi, and A.-R. Sebak, "Broadband and high-gain circularly-polarized antenna with low RCS," *IEEE Transactions on Antennas and Propagation*, Vol. 67, No. 1, 16–23, 2018.
- [10] Akbari, M., S. Zorbakhsh, F. Samadi, M. Moghadam, and A. R. Sebak, "High gain CP antenna with low RCS based on Fabry-Perot cavity," in *2018 18th International Symposium on Antenna Technology and Applied Electromagnetics (ANTEM)*, 1–2, 2018.
- [11] Zhou, Y., X. Cao, J. Gao, S. Li, and Y. Zheng, "In-band RCS reduction and gain enhancement of a dual-band PRMS-antenna," *IEEE Antennas and Wireless Propagation Letters*, Vol. 16, 2716–2720, 2017.
- [12] Zheng, Q., C. Guo, G. A. E. Vandenbosch, and J. Ding, "Low-profile circularly polarized array with gain enhancement and RCS reduction using polarization conversion EBG structures," *IEEE Transactions on Antennas and Propagation*, Vol. 68, No. 3, 2440–2445, Mar. 2020.
- [13] Zhang, L., C. Liu, C. Ni, M. Kong, and X. Wu, "Low-RCS, circular polarization, and high-gain broadband antenna based on mirror polarization conversion metasurfaces," *International Journal of Antennas and Propagation*, Vol. 2019, 6098483, Aug. 2019.
- [14] Hong, T., S. Wang, Z. Liu, and S. Gong, "RCS reduction and gain enhancement for the circularly polarized array by polarization conversion metasurface coating," *IEEE Antennas and Wireless Propagation Letters*, Vol. 18, No. 1, 167–171, Jan. 2019.
- [15] Li, K., Y. Liu, Y. Jia, and Y. J. Guo, "A circularly polarized high-gain antenna with low RCS over a wideband using chessboard polarization conversion metasurfaces," *IEEE Transactions on Antennas and Propagation*, Vol. 65, No. 8, 4288–4292, Aug. 2017.
- [16] Xie, P. and G. Wang, "Circularly polarized Fabry-Perot antenna with well RCS reduction property," *International Journal of RF and Microwave Computer-Aided Engineering*, Vol. 32, No. 12, e23527, Dec. 2022.
- [17] Liu, Z., Y. Liu, and S. Gong, "Gain enhanced circularly polarized antenna with RCS reduction based on metasurface," *IEEE Access*, Vol. 6, 46 856–46 862, 2018.
- [18] Lu, J., X. Cao, J. Gao, H. Yang, L. Jidi, and K. Gao, "High-gain and low-RCS linear polarization FP resonant cavity antenna based on metasurface," *Radioengineering*, Vol. 30, No. 4, 623, 2021.
- [19] Zheng, Y., J. Gao, Y. Zhou, X. Cao, H. Yang, S. Li, and T. Li, "Wideband gain enhancement and RCS reduction of Fabry-Perot resonator antenna with chessboard arranged metamaterial superstrate," *IEEE Transactions on Antennas and Propagation*, Vol. 66, No. 2, 590–599, Feb. 2018.
- [20] Xie, P., G.-M. Wang, H.-P. Li, Y.-W. Wang, and B. Zong, "Wideband RCS reduction of high gain Fabry-Perot antenna employing a receiver-transmitter metasurface," *Progress In Electromagnetics Research*, Vol. 169, 103–115, 2020.
- [21] Liu, Z., S. Liu, X. Zhao, X. Kong, Z. Huang, and B. Bian, "Wideband gain enhancement and RCS reduction of Fabry-Perot antenna using hybrid reflection method," *IEEE Transactions on Antennas and Propagation*, Vol. 68, No. 9, 6497–6505, Sep. 2020.
- [22] Liu, X., J. Gao, L. Xu, X. Cao, Y. Zhao, and S. Li, "A coding diffuse metasurface for RCS reduction," *IEEE Antennas and Wireless Propagation Letters*, Vol. 16, 724–727, 2016.
- [23] Su, J., C. Kong, Z. Li, H. Yin, and Y. Yang, "Wideband diffuse scattering and RCS reduction of microstrip antenna array based on coding metasurface," *Electronics Letters*, Vol. 53, No. 16, 1088–1090, 2017.
- [24] Zhuang, Y., G. Wang, J. Liang, T. Cai, X.-L. Tang, T. Guo, and Q. Zhang, "Random combinatorial gradient metasurface for broadband, wide-angle and polarization-independent diffusion scattering," *Scientific Reports*, Vol. 7, 16560, 2017.
- [25] Zhang, L., X. Wan, S. Liu, J. Y. Yin, Q. Zhang, H. T. Wu, and T. J. Cui, "Realization of low scattering for a high-gain Fabry-Perot antenna using coding metasurface," *IEEE Transactions on Antennas and Propagation*, Vol. 65, No. 7, 3374–3383, Jul. 2017.
- [26] Su, J., H. He, Z. Li, Y. Yang, H. Yin, and J. Wang, "Uneven-layered coding metamaterial tile for ultra-wideband RCS reduction and diffuse scattering," *Scientific Reports*, Vol. 8, 8182, 2018.
- [27] Fu, C., X. Zhang, X. Liu, and L. Han, "RCS reduction of composite transparent flexible coding metasurface combined phase cancellation and absorption," *Optics Express*, Vol. 31, No. 17, 27 365–27 380, 2023.